Associated charmonium production in low energy $p\bar{p}$ annihilation

T. Barnes[1,2,*] and X. Li[2,†]

[1]*Physics Division, Oak Ridge National Laboratory, Oak Ridge, Tennessee 37831, USA*
[2]*Department of Physics and Astronomy, University of Tennessee, Knoxville, Tennessee 37996, USA*
(Received 12 December 2006; published 15 March 2007)

The QCD mechanisms underlying the exclusive strong decays and hadronic production amplitudes of charmonium remain poorly understood, despite decades of study and an increasingly detailed body of experimental information. One set of hadronic channels of special interest are those that include baryon-antibaryon states. These are being investigated experimentally at BES and CLEO-c in terms of their baryon resonance content, and are also of interest for the future PANDA experiment, in which charmonium and charmonium hybrids will be produced in $p\bar{p}$ annihilation in association with light mesons. In this paper we develop a simple initial-state light meson emission model of the near-threshold associated charmonium production processes $p\bar{p} \rightarrow \pi^0 \Psi$, and evaluate the differential and total cross sections for these reactions in this model. (Here we consider the states $\Psi = \eta_c$, J/ψ, ψ', χ_0 and χ_1.) The predicted near-threshold cross section for $p\bar{p} \rightarrow \pi^0 J/\psi$ is found to be numerically similar to two previous theoretical estimates, and is roughly comparable to the (sparse) existing data for this process. The theoretical charmonium angular distributions predicted by this model are far from isotropic, which may be of interest for PANDA detector design studies.

I. INTRODUCTION

Strong decays of charmonia through annihilation of the $c\bar{c}$ pair to light hadrons dominate the total widths of the lighter charmonium states [1]. In contrast to the faster open-charm decays, which appear to be reasonably well described by both the $^3P_0$ model [2] and the Cornell time-like vector decay model [3] (given the current state of the data), the $c\bar{c}$ annihilation decays are much less well understood. There are several general rules that appear to be respected by these decays; in particular, the number of QCD vertices in the leading-order Feynman diagram for annihilation into light quarks and gluons is a useful guide. For example, the C = (+) charmonia that can annihilate at $O(g^2)$ (into gg for η_c, χ_0, χ_2, and gg for the χ_1) have strong annihilation widths of ∼1–25 MeV, often much larger than the ∼0.1–0.3 MeV widths of the C = (−) states J/ψ and ψ', which must annihilate at $O(g^3)$ into ggg. Since $c\bar{c}$ annihilation is a short-ranged process (the charm quark propagator implies a range of $r \sim 1/m_c$), a strong suppression of annihilation widths with increasing orbital angular momentum $L_{c\bar{c}}$ is also anticipated; this suggests, for example, that the D-wave $c\bar{c}$ states $^1D_2$ and $^3D_2$, if below their DD* open-charm threshold, will have strong widths of <1 MeV [3,4].

Although the inclusive annihilation decays are qualitatively understood in terms of $c\bar{c}$ annihilation into gluons, exclusive $c\bar{c}$ annihilation decays remain a mystery, despite the existence of considerable experimental information on the branching fractions of some $c\bar{c}$ states into specific exclusive modes. In particular, much is known about the

exclusive two-body annihilation decays of the J/ψ and ψ', and a "12% rule" for the relative branching fractions of the ψ' and J/ψ into many of these modes is part of charmonium folklore. The recent increase in the number of modes studied, for example, by CLEO-c [5], has made it clear however that this rule is not generally applicable.

In this paper we note that there may be a simple relation between some two-body and three-body annihilation decays of charmonia, specifically in decays to the final states $p\bar{p}$ and $p\bar{p}\pi^0$. These decays are of interest both as a novel technique for studying N* spectroscopy, for example, at BES [6–9] and because they can be used to estimate the cross sections for associated charmonium production in $p\bar{p}$ annihilation, as in $p\bar{p} \rightarrow \pi^0 + \Psi$ [10]. (We use Ψ to represent a generic charmonium state.) These cross sections are of particular interest in that they will be exploited by the PANDA project at GSI [11] to search for excited charmonia and charmonium hybrids. The scales of these cross sections are at present largely unknown; a better understanding of these associated charmonium production processes near threshold is obviously crucial for planning various aspects of this experiment, such as detector design and data acquisition.

II. THE MODEL

A. Motivation

Since strong decays to three-body final states are typically dominated by quasi-two-body transitions, one might anticipate that decays of the type $\Psi \rightarrow p\bar{p}\pi^0$ could be described as two-step processes, $\Psi \rightarrow (N^{*+}\bar{p} + H.c.) \rightarrow p\bar{p}\pi^0$, where the important N* baryon isobars are those with large Nπ couplings. Specifically we might expect the nucleon itself to make a large or perhaps dominant con-

*Electronic address: tbarnes@utk.edu
†Electronic address: xli22@utk.edu

tribution, in view of the large $NN\pi$ coupling. This in turn suggests that the associated production of a Ψ state and a pion in $p\bar{p}$ annihilation may take place through initial emission of a pion from the incoming p or $\bar{p}$ line, followed by direct annihilation of the $p\bar{p}$ state into $c\bar{c}$. At tree level this process is described by the two Feynman diagrams of Fig. 1.

The use of these simple hadron-level "pole" diagrams to describe these processes was previously suggested by Gaillard, Maiani and Petronzio [12], who considered the production of charmonium from $p\bar{p}$ states with specified initial quantum numbers in a PCAC model. Their work was subsequently extended analytically by Lundborg, Barnes and Wiedner [10] (much of Ref. [12] was numerical). Lundborg *et al.* also showed that a constant amplitude approximation could be used to estimate the cross section for $p\bar{p} \rightarrow \pi^0\Psi$ from the corresponding three-body decay $\Psi \rightarrow p\bar{p}\pi^0$; numerical results for $\sigma(p\bar{p} \rightarrow \pi^0 J/\psi)$ using both approaches are given in that reference.

The work presented here gives extensive analytic results for differential and total cross sections derived from the pole model, assuming plane wave initial $p\bar{p}$ states. If the partial width of a charmonium state Ψ to $p\bar{p}$ is known experimentally, one can use this to estimate the corresponding $\Psi - p\bar{p}$ coupling constant $g_{p\bar{p}\Psi}$. Since the $NN\pi$ coupling constant is known, one may then evaluate the differential and total cross sections for $p\bar{p} \rightarrow \pi^0\Psi$ both analytically and numerically in this model. Here we carry out this exercise for the cases of five low-lying Ψ states with known $p\bar{p}$ partial widths, specifically the η_c, J/ψ, ψ', χ_0 and χ_1.

B. Amplitudes

We describe the reactions $p\bar{p} \rightarrow \pi^0\Psi$ as two-step processes, initial pion emission from an incident proton or antiproton followed by direct annihilation of the proton-antiproton pair, $p\bar{p} \rightarrow \Psi$. This process at tree level is described by the two Feynman diagrams of Fig. 1. The $pp\pi^0$ and $\bar{p}\,\bar{p}\,\pi^0$ vertices are taken to be the usual $g_{pp\pi}\gamma_5$, and the $p\bar{p}\Psi$ vertex is generically $g_{p\bar{p}\Psi}\Gamma$, where the Dirac matrix Γ specifies the quantum numbers of the state Ψ. We use $\Gamma = \gamma_5$ for the η_c, $-i$ for the χ_0, $-i\gamma_\mu$ for the J/ψ and ψ', and $-i\gamma_\mu\gamma_5$ for the χ_1. For the vector and axial-vector cases J/ψ, ψ' and χ_1, Γ is implicitly contracted into the final Ψ polarization four-vector ϵ_μ^*. Of course in general one will have hadronic form factors at all these vertices, and more complicated Lorentz structures (such as $\sigma_{\mu\nu}q_\nu$
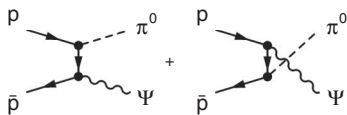
for the J/ψ) can be formed if one allows derivative couplings. As data from PANDA becomes available it will be of interest to consider these more general forms; for this first estimate we assume the simplest possible vertices, which are the minimal Dirac matrices times fixed coupling constants.

The invariant amplitude for $p\bar{p} \rightarrow \pi^0\Psi$ in this model is

$$\mathcal{M} = ig_\pi g_\Psi \bar{v}_{\bar{p}\,\bar{s}} \left[\Gamma \frac{(\not{p} - \not{k} + m)}{(t - m^2)} \gamma_5 \right.$$
$$\left. + \gamma_5 \frac{(\not{k} - \bar{\not{p}} + m)}{(u - m^2)} \Gamma \right] u_{ps}. \quad (1)$$

Here and in the following expressions m is the proton mass, m_π is the pion mass, M is the mass of the charmonium state Ψ, and $r_\pi = m_\pi/m$ and $r_\Psi = M/m$ are dimensionless mass ratios relative to the proton. The pion-nucleon coupling constant is $g_\pi \equiv g_{pp\pi}$, and the (state-dependent) charmonium-$p\bar{p}$ coupling constant is $g_\Psi \equiv g_{p\bar{p}\Psi}$. We also define squared strong coupling constants $\alpha_\pi \equiv g_{pp\pi}^2/4\pi$ and $\alpha_\Psi \equiv g_{p\bar{p}\Psi}^2/4\pi$.

It is sometimes useful to rewrite this invariant amplitude in an equivalent form that makes the overall $t \leftrightarrow u$ crossing symmetry more evident;

$$\mathcal{M} = -\frac{ig_\pi g_\Psi/2}{(t - m^2)(u - m^2)} \cdot [(s - M^2 - m_\pi^2)\bar{v}_{\bar{p}\,\bar{s}}\{\gamma_5\not{k}, \Gamma\}u_{ps}$$
$$- (t - u)\bar{v}_{\bar{p}\,\bar{s}}[\gamma_5\not{k}, \Gamma]u_{ps}]. \quad (2)$$

Since the commutator (anticommutator) of $\gamma_5\not{k}$ with Γ vanishes for scalar (pseudoscalar) Ψ, this rearrangement simplifies the calculation considerably in these cases.

C. Massless pions

1. Differential cross sections

The differential and total cross sections we find given this invariant amplitude are rather simple in the massless pion limit, and only involve two independent functions. For this reason we first give results for massless pions, and then treat each set of charmonium quantum numbers separately for nonzero pion mass. Our results for the unpolarized differential cross sections in the massless pion limit are

$$\left\langle \frac{d\sigma}{dt} \right\rangle \bigg|_{p\bar{p}\rightarrow\pi^0\eta_c} = \frac{\pi}{2} \frac{\alpha_\pi\alpha_\Psi}{s(s - 4m^2)} \frac{(x - y)^2}{xy}, \quad (3)$$

$$\left\langle \frac{d\sigma}{dt} \right\rangle \bigg|_{p\bar{p}\rightarrow\pi^0\chi_0} = \frac{1}{2} \left\langle \frac{d\sigma}{dt} \right\rangle \bigg|_{p\bar{p}\rightarrow\pi^0(J/\psi,\psi')}$$
$$= \frac{\pi}{2} \frac{\alpha_\pi\alpha_\Psi}{s(s - 4m^2)} \frac{f^2}{xy}, \quad (4)$$

FIG. 1. Feynman diagrams assumed in this model of the generic reaction $p\bar{p} \rightarrow \pi^0\Psi$.

$$\left\langle \frac{d\sigma}{dt} \right\rangle \Bigg|_{p\bar{p} \to \pi^0 \chi_1} = \pi \frac{\alpha_\pi \alpha_\Psi}{s(s - 4m^2)} \cdot \left[(1 - 2/r_\Psi^2) \frac{f^2}{xy} \right.$$

$$\left. + 2(r_\Psi^2 f - 1) \right]. \qquad (5)$$

Here x and y are dimensionless, shifted Mandelstam variables $x \equiv t/m^2 - 1$ and $y \equiv u/m^2 - 1$, and f is a dimensionless energy variable, which for general masses is given by $f = (s - m_\pi^2 - M^2)/m^2 = -(x + y)$.

There are several interesting features in these angular distributions which are relevant to PANDA. Note that the differential cross sections in Eqs. (3)–(5) are $t \leftrightarrow u$ ($x \leftrightarrow y$) crossing symmetric, and that there are maxima in the forward and backwards directions, which give the largest values for the proton propagator functions $1/|t - m^2| = 1/m^2|x|$ and $1/|u - m^2| = 1/m^2|y|$. A more striking effect is the zero in the angular distribution of the final state $\pi^0 \eta_c$, which follows from the odd $t \leftrightarrow u$ spatial symmetry of this amplitude; this implies a node at $t = u$, corresponding to $\theta = \pi/2$ in the c.m. frame. In comparison the angular distributions of the other final states we consider also have minima at $t = u$, but are nonzero there. These rapidly varying angular distribution could be used to test for the presence of this signal over the presumably more slowly varying backgrounds.

2. Total cross sections

In the massless pion limit the unpolarized total cross sections follow from integrating the results in Eqs. (3)–(5) over t. They may conveniently be written as functions of s and $\beta = \sqrt{1 - 4m^2/s}$ (the p or $\bar{p}$ velocity in the c.m. frame), and are given by

$$\langle \sigma \rangle|_{p\bar{p} \to \pi^0 \eta_c} = 2\pi \alpha_\pi \alpha_\Psi \frac{(s - M^2)}{s^2 \beta^2} [\tanh^{-1}\beta - \beta] \quad (6)$$

$$\langle \sigma \rangle|_{p\bar{p} \to \pi^0 \chi_0} = 2\pi \alpha_\pi \alpha_\Psi \frac{(s - M^2)}{s^2 \beta^2} \tanh^{-1}\beta \qquad (7)$$

$$\langle \sigma \rangle|_{p\bar{p} \to \pi^0 \chi_1} = 2\pi \alpha_\pi \alpha_\Psi \frac{(s - M^2)}{s^2 \beta^2} \cdot [2(1 - 2/r_\Psi^2)\tanh^{-1}\beta$$
$$+ (s/M^2 - 2)\beta]. \qquad (8)$$

The massless pion total cross section formulas for the final states $\pi^0 J/\psi$ and $\pi^0 \psi'$ are proportional to the $\pi^0 \chi_0$ result, as implied by Eq. (4); $\sigma(J/\psi) = \sigma(\psi') = 2\sigma(\chi_0)$. We stress that these simple ratios only apply to the algebraic expressions; the actual numerical cross sections are not simply related, due to a) different kinematics, and b) the strongly state-dependent $g_{p\bar{p}\Psi}$ couplings, which are given in Table I.

TABLE I. Charmonium-$p\bar{p}$ coupling constants, estimated from the measured branching fractions and total widths [1] and the $\Gamma_{\Psi \to p\bar{p}}$ width formulas of Eqs. (26)–(29) (see text).

State Ψ	$B_{\Psi \to p\bar{p}}$	$\Gamma_\Psi^{\text{tot.}}$ [MeV]	$10^3 \cdot g_{p\bar{p}\Psi}$
η_c	$(1.3 \pm 0.4) \cdot 10^{-3}$	25.5 ± 3.4	19.0 ± 3.2
J/ψ	$(2.17 \pm 0.08) \cdot 10^{-3}$	0.0934 ± 0.0021	1.62 ± 0.03
ψ'	$(2.65 \pm 0.22) \cdot 10^{-4}$	0.337 ± 0.013	0.97 ± 0.04
χ_0	$(2.24 \pm 0.27) \cdot 10^{-4}$	10.4 ± 0.7	5.42 ± 0.37
χ_1	$(6.7 \pm 0.5) \cdot 10^{-5}$	0.89 ± 0.05	1.03 ± 0.07
χ_2	$(6.6 \pm 0.5) \cdot 10^{-5}$	2.06 ± 0.12	$\cdots$

D. Massive pions

1. Kinematics

The results given in the previous section for massless pions are attractive in their simplicity, and are useful for numerical estimates well above threshold. However we find that the angular distributions near threshold are strongly dependent on the pion mass (the massless case is a singular limit), and the difference in the location of the threshold for massless versus massive pions leads to numerically important differences in the predicted cross sections at energies relevant to PANDA. For these reasons we give detailed predictions for the differential and total cross sections for these charmonium production processes in the case of general pion mass.

Since we will discuss some angular distributions in the c.m. frame, it is useful to have the relation between Mandelstam variables and proton (p) and pion (k) variables in this frame for general masses. These relations are

$$E_p = \frac{s^{1/2}}{2} \qquad (9)$$

$$p = \frac{s^{1/2}}{2}\left(1 - \frac{4m^2}{s}\right)^{1/2} \qquad (10)$$

$$E_k = \frac{s^{1/2}}{2}\left(1 - \frac{(M^2 - m_\pi^2)}{s}\right) \qquad (11)$$

$$k = \frac{s^{1/2}}{2}\left(1 - \frac{2(M^2 + m_\pi^2)}{s} + \frac{(M^2 - m_\pi^2)^2}{s^2}\right)^{1/2} \qquad (12)$$

2. Differential cross sections

For general pion mass the differential cross sections $\{\langle d\sigma/dt \rangle\}$ may be written as multiplier functions $\{F_\Psi\}$ times the massless pion formulas of Eqs. (3)–(5). These functions, expressed as power series in $r_\pi = m_\pi/m$, are

$$F_{\eta_c} = 1 - \frac{r_\Psi^2}{xy} r_\pi^2 \qquad (13)$$

$$F_{\chi_0} = 1 - \frac{(r_\Psi^2 - 4)}{xy} r_\pi^2 \qquad (14)$$

$$F_{J/\psi,\psi'} = 1 + \left(\frac{2(r_\Psi^2 + f)}{f^2} - \frac{(r_\Psi^2 + 2)}{xy}\right) r_\pi^2 + \frac{2}{f^2} r_\pi^4. \quad (15)$$

In the χ_1 case it is simpler to give the full differential cross section with nonzero pion mass directly. This result is

$$\left\langle \frac{d\sigma}{dt} \right\rangle \bigg|_{p\bar{p} \to \pi^0 \chi_1} = \pi \frac{\alpha_\pi \alpha_\Psi}{s(s - 4m^2)} \cdot \left\{ \left[2(f/r_\Psi^2 - 1) \right. \right.$$
$$\left. + \frac{(1 - 2/r_\Psi^2)f^2}{xy} \right]$$
$$+ \left[\frac{2}{r_\Psi^2} + \frac{2(r_\Psi^2 - f - 4)}{xy} - \frac{(r_\Psi^2 - 4)f^2}{(xy)^2} \right] r_\pi^2$$
$$\left. - \frac{2}{xy} r_\pi^4 \right\}. \qquad (16)$$

Examples of these angular distributions will be shown in the section on numerical results.

3. Total cross sections

In the case of general masses, inspection of the differential cross sections implied by Eqs. (3)–(5) and Eqs. (13)–(15) shows that the total cross sections may all be evaluated analytically in terms of integrals over x, which are generically of the form

$$I_m = \int_{x_0}^{x_1} \frac{dx}{(xy)^m} \qquad (17)$$

where $y = -x - f$. The limits of integration are implied by the definition $x = t/m^2 - 1$, and in terms of proton (p) and pion (k) c.m. frame energies and three-momenta are

$$x_{\substack{1 \\ 0}} = (m_\pi^2 - 2E_p E_k \pm 2pk)/m^2. \qquad (18)$$

These limits may also be written in terms of masses and the Mandelstam variable s, using the relations given in Eqs. (9)–(12). The explicit indefinite integrals required for our cross section calculations are

$$I_0(x) = x \qquad (19)$$

$$I_1(x) = \frac{1}{f} \ln\left(\frac{x + f}{x}\right) \qquad (20)$$

$$I_2(x) = \frac{2}{f^3} \ln\left(\frac{x + f}{x}\right) - \frac{1}{f^2}\left(\frac{1}{x + f} + \frac{1}{x}\right). \qquad (21)$$

In terms of these integrals, evaluated between the limits x_0 and x_1 (so that $I_m \equiv I_m(x_1) - I_m(x_0)$), the total cross sections are

$$\langle \sigma \rangle_{p\bar{p} \to \pi^0 \eta_c} = \frac{\pi \alpha_\pi \alpha_\Psi}{2} \frac{m^2}{s(s - 4m^2)} \cdot \left[-(4I_0 - f^2 I_1) \right.$$
$$\left. + r_\pi^2 r_\Psi^2 (4I_1 - f^2 I_2) \right] \qquad (22)$$

$$\langle \sigma \rangle_{p\bar{p} \to \pi^0 (J/\psi,\psi')} = \pi \alpha_\pi \alpha_\Psi \frac{m^2}{s(s - 4m^2)}$$
$$\cdot \left[f^2 I_1 + r_\pi^2 (2(r_\Psi^2 + f) I_1 \right.$$
$$- (r_\Psi^2 + 2) f^2 I_2) + r_\pi^4 2 I_1 \right] \qquad (23)$$

$$\langle \sigma \rangle_{p\bar{p} \to \pi^0 \chi_0} = \frac{\pi \alpha_\pi \alpha_\Psi}{2} \frac{m^2 f^2}{s(s - 4m^2)} [I_1 - r_\pi^2 (r_\Psi^2 - 4) I_2] \qquad (24)$$

$$\langle \sigma \rangle_{p\bar{p} \to \pi^0 \chi_1} = \pi \alpha_\pi \alpha_\Psi \frac{m^2}{s(s - 4m^2)} \cdot \left[(2(f/r_\Psi^2 - 1) I_0 \right.$$
$$+ f^2 (1 - 2/r_\Psi^2) I_1)$$
$$+ r_\pi^2 (2/r_\Psi^2 I_0 + 2(r_\Psi^2 - f - 4) I_1$$
$$\left. - f^2 (r_\Psi^2 - 4) I_2) - r_\pi^4 2 I_1 \right]. \qquad (25)$$

These cross sections will be evaluated numerically in the next section.

III. NUMERICAL RESULTS

A. Estimating the $p\bar{p}\Psi$ coupling constants

Numerical evaluation of our predictions for cross sections and related quantities requires values for the model parameters. The hadron masses are of course well known, as is the NNπ coupling constant $g_\pi \equiv g_{pp\pi}$, which we take to be 13.5. The coupling strengths of the various charmonium resonances to $p\bar{p}$ however are not well established; this is a crucial issue for the PANDA project, which assumes that these couplings are sufficiently large to allow the accumulation of large charmonium event samples in $p\bar{p}$ annihilation.

Since the partial widths of several charmonium states to $p\bar{p}$ are now known experimentally, one may estimate these state-dependent charmonium-$p\bar{p}$ coupling constants $\{g_\Psi\}$ by equating the measured partial widths to the $O(g_\Psi^2)$ theoretical partial widths we calculate in our model, assuming the same pointlike $p\bar{p}\Psi$ vertices that we used to calculate the $p\bar{p} \to \pi^0 \Psi$ cross sections. In terms of the $\alpha_\Psi = g_{p\bar{p}\Psi}^2/4\pi$ and the final p velocity $\beta = \sqrt{1 - 4m^2/M^2}$, these partial widths are

$$\Gamma(\eta_c \to p\bar{p}) = \alpha_{\eta_c} \beta M/2 \qquad (26)$$

$$\Gamma(J/\psi \to p\bar{p}) = \alpha_{J/\psi} \beta (1 + 2/r_\Psi^2) M/3 \qquad (27)$$

$$\Gamma(\chi_0 \to p\bar{p}) = \alpha_{\chi_0} \beta^3 M/2 \qquad (28)$$

$$\Gamma(\chi_1 \to p\bar{p}) = \alpha_{\chi_1}\beta^3 M/3. \qquad (29)$$

We use these relations and the measured branching fractions and total widths to estimate values for the various charmonium-$p\bar{p}$ coupling constants; these results are shown in Table I. Note that the couplings of the pseudoscalar and scalar states η_c and χ_0 to $p\bar{p}$ are an order of magnitude larger than the couplings of the vector and axial-vector states.

B. Total cross sections

We will now evaluate the total unpolarized cross sections $\langle\sigma\rangle(p\bar{p} \to \pi^0\Psi)$ for the five cases $\Psi = \eta_c, J/\psi, \chi_0,$ χ_1 and ψ', using the formulas given in Eqs. (22)–(25). The masses assumed are 2006 PDG values [1] rounded to 0.1 MeV; $m_{\pi^0} = 0.1350$ GeV, $m_p = 0.9383$ GeV, $M_{\eta_c} = 2.9804$ GeV, $M_{J/\psi} = 3.0969$ GeV, $M_{\chi_0} = 3.4148$ GeV, $M_{\chi_1} = 3.5107$ GeV and $M_{\psi'} = 3.6861$ GeV. The $pp\pi^0$ coupling constant is taken to be $g_\pi = 13.5$, and the $p\bar{p}\Psi$ couplings are given in Table I. The resulting cross sections are shown in Fig. 2. The E760 and E835 data for the $p\bar{p} \to \pi^0 J/\psi$ total cross section near 3.5 GeV (also shown in Fig. 2) suggest that our results overestimate this cross section at this E_{cm} by about a factor of 2.

Evidently these cross sections share a rapid rise above threshold, followed by a slowly varying "plateau" region above $E_{cm} \approx 4$ GeV. The most remarkable feature may be the wide variation in the plateau values with the charmonium state Ψ. The largest cross section by far is for η_c production, which is roughly a factor of 30 larger than the J/ψ cross section. Second is the χ_0 cross section, roughly 5 times larger than J/ψ. Since the χ_0 has a radiative branching fraction to $\gamma J/\psi$ of $35.6 \pm 1.9\%$, this implies
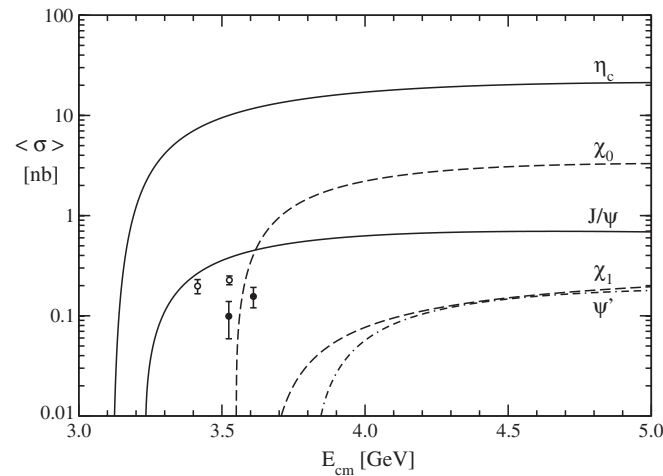
that J/ψ production through the radiative process $p\bar{p} \to \pi^0\chi_0,$ $\chi_0 \to \gamma J/\psi$ is comparable to the direct process $p\bar{p} \to \pi^0 J/\psi$. Finally, the χ_1 and ψ' cross sections are smaller than the J/ψ by about a factor of 5–10. (For the ψ' to J/ψ ratio this is reminiscent of the 12% rule for a radial excitation.) These results suggest that the associated production of charmonium and charmonium hybrids with certain quantum numbers is strongly enhanced in $p\bar{p}$ production, and that $J^{PC} = 0^{-+}$ and 0^{++} states may be the most favored.

C. Angular distributions

The angular distributions predicted by this model of $p\bar{p} \to \pi^0\Psi$ are especially interesting, since they are far from isotropic and may be important for design of the PANDA detector. Two representative cases for $\langle d\sigma/d\Omega\rangle$ (c.m. frame) are shown in the figures; both show angular distributions normalized to unity in the forward direction, with E_{cm} in steps of 0.2 GeV up to a cutoff of $E_{cm} = 5.0$ GeV. The contours at $E_{cm} = 4.0$ GeV and $E_{cm} = 5.0$ GeV are highlighted.

The first angular distribution, in Fig. 3, shows the prediction of Eqs. (4) and (15) for the reaction $p\bar{p} \to \pi^0 J/\psi$. This distribution is isotropic as we approach threshold, but with increasing E_{cm} evidently becomes strongly forward- and backward-peaked. (All the unpolarized cross sections we consider are front-back symmetric.)

The second angular distribution is for the reaction $p\bar{p} \to \pi^0\eta_c$, which is predicted to be the largest associated charmonium production cross section by a considerable margin. This angular distribution, taken from Eqs. (3) and (13), is shown in Fig. 4. (The same conventions are used as in the previous figure.) This differential cross section shows a similar forward- and backward-peaking with increasing E_{cm}, and has in addition a very characteristic node at $t = u$, which is $\theta = 90^o$ in the c.m. frame. The large
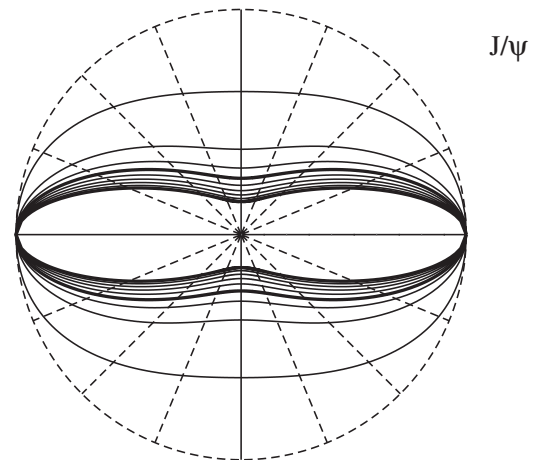

FIG. 2. Predicted unpolarized total cross sections for the processes $p\bar{p} \to \pi^0\Psi$, where $\Psi = \eta_c, J/\psi, \chi_0, \chi_1$ and ψ'. The data points are Fermilab measurements of the cross section for $p\bar{p} \to \pi^0 J/\psi$, from E760 [14] (filled) and E835 [15] (open). There are additional experimental results for this reaction from E835 [16] which have not yet been published as a physical cross section.

FIG. 3. Predicted c.m. frame unpolarized angular distribution $\langle d\sigma/d\Omega\rangle$ for the process $p\bar{p} \to \pi^0 J/\psi$, normalized to the forward intensity, for $E_{cm} = 3.4$–5.0 GeV in steps of 0.2 [GeV].

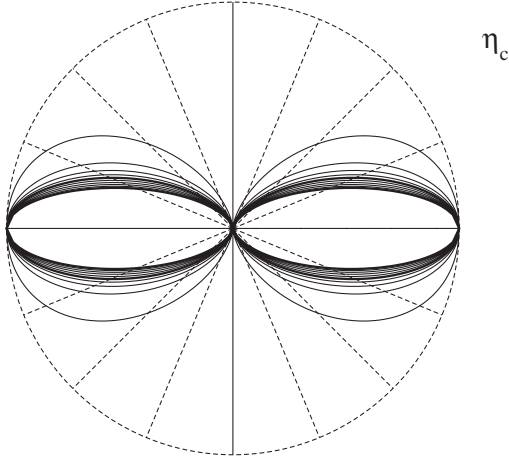FIG. 4. The corresponding angular distribution for the reaction $p\bar{p} \rightarrow \pi^0 \eta_c$, for E_{cm} = 3.2–5.0 GeV in steps of 0.2 [GeV].

overall scale of this cross section suggests that the detection of unusual modes such as $p\bar{p} \rightarrow 4\gamma$ may be feasible (with both the π^0 and η_c decaying to $\gamma\gamma$).

IV. SUMMARY AND FUTURE

In this paper we have developed a hadronic pole model of charmonium production with an associated pion in proton-antiproton collisions. Given the Feynman diagrams of Fig. 1 we derived closed-form analytic results for the unpolarized differential and total cross sections for the processes $p\bar{p} \rightarrow \pi^0\Psi$, where the quantum numbers considered for the charmonium state Ψ were 0^{-+}, 0^{++}, 1^{--} and 1^{++}. We quoted results for both massless and massive pions.

Besides the hadron masses this model has as free parameters the known $g_{pp\pi^0}$ and the coupling $g_{p\bar{p}\Psi}$ of the specified charmonium state Ψ to $p\bar{p}$. Here we used the experimental partial widths of light charmonium states to $p\bar{p}$ to estimate the coupling constants $\{g_{p\bar{p}\Psi}\}$. Given this information we numerically evaluated the differential and total cross sections for these reactions. In particular we gave numerical predictions for the total cross section for the cases $\Psi = \eta_c$, J/ψ, χ_0, χ_1 and ψ' (Fig. 2), and for the differential cross sections in two representative cases, $\Psi = J/\psi$ (Fig. 3) and η_c (Fig. 4).

The total cross sections predicted for the production of other charmonium states than the J/ψ are especially interesting. The reaction $p\bar{p} \rightarrow \pi^0\eta_c$ is predicted to have the largest cross section by a considerable margin, followed by the χ_0. The two smallest cross sections are predicted for the χ_1 and ψ'. These results suggest that $J^{PC} = 0^{-+}$ and

0^{++} charmonium states may be the most copiously produced in the PANDA experiment. A comparison of the J/ψ and ψ' suggests that the first radial excitation cross sections are suppressed relative to the ground states by about a factor of 5–10 in the relevant PANDA energy regime.

Several future developments related to this type of model appear especially interesting. The important question of the size of the associated production cross sections of other charmonium states can be answered in this model given their $p\bar{p}$ branching fractions, so $B_{p\bar{p}}$ is a very important measurements for the charmonium states we have not considered here. Similarly, the cross sections for emission of a charmonium state Ψ accompanied by other light mesons $\{m\}$ can be studied; this may also be used to clarify poorly known ppm couplings. The importance of initial and final polarizations, which may be accessible at PANDA, can easily be addressed in this model. An important effect which has not been included is the contribution of intermediate N^* resonances to the $p\bar{p} \rightarrow \pi^0\Psi$ transition amplitudes; the $NN^*\Psi$ couplings can be extracted from the corresponding $\Psi \rightarrow NN^*$ decays. It would also be of interest to determine the effect of replacing the pseudoscalar $pp\pi^0$ coupling we have assumed here by the axial-vector PCAC form, as this may significantly modify the predicted cross sections in the soft pion limit [13]. The large value of the coupling constant $g_{pp\pi}$ suggests that higher-order processes such as $p\bar{p} \rightarrow \pi\pi\Psi$ may be important in this model; this would also be an interesting calculation, and in the simple nucleon pole model requires no additional parameters. Finally, as our approximation of pointlike hadron vertices is unrealistic well above threshold, it would be very interesting to study the effect of plausible $pp\pi^0$ and $p\bar{p}\Psi$ form factors on our results.

[1] W.-M. Yao *et al.*, J. Phys. G **33**, 1 (2006).
[2] T. Barnes, S. Godfrey, and E. S. Swanson, Phys. Rev. D **72**,

054026 (2005).
[3] E. J. Eichten, K. Lane, and C. Quigg, Phys. Rev. D **69**,

094019 (2004).

[4] T. Barnes and S. Godfrey, Phys. Rev. D **69**, 054008 (2004).

[5] R. A. Briere *et al.* (CLEO-c Collaboration), Phys. Rev. Lett. **95**, 062001 (2005).

[6] J. Z. Bai *et al.* (BES Collaboration), Phys. Lett. B **510**, 75 (2001).

[7] M. Ablikim *et al.* (BES Collaboration), Phys. Rev. Lett. **97**, 062001 (2006).

[8] M. Ablikim *et al.* (BES Collaboration), Phys. Rev. D **71**, 072006 (2005).

[9] W. H. Liang, P. N. Shen, B. S. Zou, and A. Faessler, Eur. Phys. J. A **21**, 487 (2004).

[10] A. Lundborg, T. Barnes, and U. Wiedner, Phys. Rev. D **73**, 096003 (2006).

[11] Technical Progress Report for: P̄ANDA, Strong Interaction Studies with Antiprotons (Feb. 2005).

[12] M. K. Gaillard, L. Maiani, and R. Petronzio, Phys. Lett. B **110**, 489 (1982).

[13] W. Weise (private communication).

[14] T. A. Armstrong *et al.*, Phys. Rev. Lett. **69**, 2337 (1992).

[15] D. N. Joffe, hep-ex/0505007.

[16] M. Andreotti *et al.*, Phys. Rev. D **72**, 032001 (2005).